

The following resources related to this article are available online at www.sciencemag.org (this information is current as of October 16, 2009):

Updated information and services, including high-resolution figures, can be found in the online version of this article at:

<http://www.sciencemag.org/cgi/content/full/326/5951/408>

A list of selected additional articles on the Science Web sites **related to this article** can be found at:

<http://www.sciencemag.org/cgi/content/full/326/5951/408#related-content>

This article **cites 19 articles**, 2 of which can be accessed for free:

<http://www.sciencemag.org/cgi/content/full/326/5951/408#otherarticles>

This article has been **cited by** 1 articles hosted by HighWire Press; see:

<http://www.sciencemag.org/cgi/content/full/326/5951/408#otherarticles>

This article appears in the following **subject collections**:

Physics, Applied

http://www.sciencemag.org/cgi/collection/app_physics

Information about obtaining **reprints** of this article or about obtaining **permission to reproduce this article** in whole or in part can be found at:

<http://www.sciencemag.org/about/permissions.dtl>

The Packing of Granular Polymer Chains

Ling-Nan Zou,^{1*} Xiang Cheng,^{1,2} Mark L. Rivers,³ Heinrich M. Jaeger,¹ Sidney R. Nagel¹

Rigid particles pack into structures, such as sand dunes on the beach, whose overall stability is determined by the average number of contacts between particles. However, when packing spatially extended objects with flexible shapes, additional concepts must be invoked to understand the stability of the resulting structure. Here, we examine the disordered packing of chains constructed out of flexibly connected hard spheres. Using x-ray tomography, we find that long chains pack into a low-density structure whose mechanical rigidity is mainly provided by the backbone. On compaction, randomly oriented, semi-rigid loops form along the chain, and the packing of chains can be understood as the jamming of these elements. Finally, we uncover close similarities between the packing of chains and the glass transition in polymers.

It is an enduring puzzle why a boxful of ball bearings, even when compacted by many taps, never packs denser than ≈ 0.64 (1–6). This is much less dense than Kepler’s stacking of triangular layers, known to every grocer as the optimal packing of oranges (packing density ≈ 0.74). Yet despite their suboptimal density and lack of periodic order, jammed packings are rigid and resist shear. Replacing spheres with less symmetric objects (such as rods or ellipsoids) introduces new degrees of freedom that alter the packing structure and create new modes of response (7–12). Here, we describe the jammed packing of flexible granular chains. Although density and coordination number decrease dramatically with increasing chain length, the packings remain rigid. Using x-ray tomography to visualize the chain conformations, we find that long floppy chains effectively partition into a collection of nearly rigid elements—small loops—that then jam into a rigid packing. Randomly packed spheres have often been used as a model for simple glasses (2, 13). Building on this result and also on the fact that polymer molecules are often modeled as flexible chains (14, 15), we find that the jammed packing of chains captures the dependence of the polymer glass transition on chain length, topology, and stiffness.

Our chains are the familiar ball-chains commonly used as window shade pulls (Fig. 1B, inset image): The “monomers” are hollow metal spheres, and the “bonds” are short metal rods. The monomers are uniform in size and evenly distributed along the chain; they are also free to rotate about the backbone so that the chain does not support torsion. These ball-chains are not arbitrarily flexible: There is a maximum bond-flex angle θ_{\max} . We use the minimum loop size $\xi = 2\pi/\theta_{\max}$ as a simple measure of chain stiffness; this is the minimum length of chain that can close to form a ring. We used an aluminum chain with monomer diameter $a = 2.4$ mm and $\xi = 7.5$, as well as a brass chain with $a =$

1.9 mm and $\xi = 11.2$. For each, we studied the packing of linear chains with free ends and of cyclic chains whose ends are connected together in a loop.

The chains are loaded into a cylindrical cell mounted on an electro-mechanical shaker: Long chains are rapidly unspooled into the cell end-first; short chains are poured in a few at a time. The chains are compacted by giving the cell discrete vertical “taps”: a single period of 30-Hz sinusoidal vibration with peak-to-peak acceleration of $8g$, where $g = 9.8$ m/s². After each tap, the pack height is measured to find the packing density ρ . The compaction dynamics of chains is similar to that of hard spheres (6): ρ increases in a logarithmic fashion with the number of taps and is slow to approach a steady state; we chose 10^4 taps as an arbitrary stopping point to measure the “final” density ρ_f . The packing produced is always disordered with no signs of chain crystallization. We repeated these measurements using cells of two different diameters (4.75 and 2.5 cm); this had no strong effect on our results.

Figure 1A plots ρ_f versus M , which is the number of monomers per chain. For linear chains, ρ_f falls monotonically with increasing M , from $\rho_f \approx 0.64$ for $M = 1$ to a much-reduced asymptotic value $\rho_{f,\infty}$ for the longest chains ($M \rightarrow \infty$). The asymptotic density is slightly higher for the floppy chain

($\xi = 7.5$ and $\rho_{f,\infty} = 0.43$) than for the stiff chain ($\xi = 11.2$ and $\rho_{f,\infty} = 0.39$). For linear chains, variation in M changes the density of chain ends in the pack. For cyclic chains, end effects are absent. As expected, long cyclic and linear chains pack at the same asymptotic density; however, short (but still floppy) cyclic chains ($M \geq 2\xi$) also packs at $\rho_{f,\infty}$. Still smaller ($M \rightarrow \xi$), semi-rigid cyclic chains actually pack less densely than the long chain limit. The trend in cyclic chains is opposite that found in linear chains, where short chains pack denser than long ones.

The observation that small, floppy cyclic chains pack at $\rho_{f,\infty}$ suggests that end effects are responsible for the enhanced packing density of short linear chains (in the floppy regime). We can check this directly by packing a mixture of linear and cyclic chains of the same length. As shown in Fig. 1B, ρ_f increases linearly with the fraction of linear chains. This indicates that in a packing of floppy chains, ends act as non-interacting, density-enhancing defects.

To reveal the detailed packing structure, we used x-ray tomography. Only the $\xi = 7.5$ Al chain is sufficiently x-ray transparent to be imaged. Our x-ray source is a 37-keV beam (GSECARS beam line) at the Argonne Advanced Photon Source. The beam size limits us to a relatively small sample: The chains are confined inside a cylinder of diameter 2.5 cm (≈ 10.5 monomer diameters), and the imaging volume covers 5 cm (out of ≈ 20 cm) of the packing column, containing 1000 to 1500 monomers. On the other hand, the high image resolution (27.5 μm per voxel) allows us to accurately locate every monomer and trace every bond.

Figure 2A shows the pair distribution function $g(r)$ for packings of linear chains from $M = 1$ to 4096. The most notable change with M is in the structure of the second peak, associated with second-nearest neighbors. For spheres ($M = 1$), the second peak of $g(r)$ is split into two subpeaks, a well-known feature corresponding to two distinct particle arrangements (16). The subpeak at $r/a = 2$ corresponds to a linear trimer; for chains, this configuration naturally suggests three successive monomers along a backbone. The subpeak

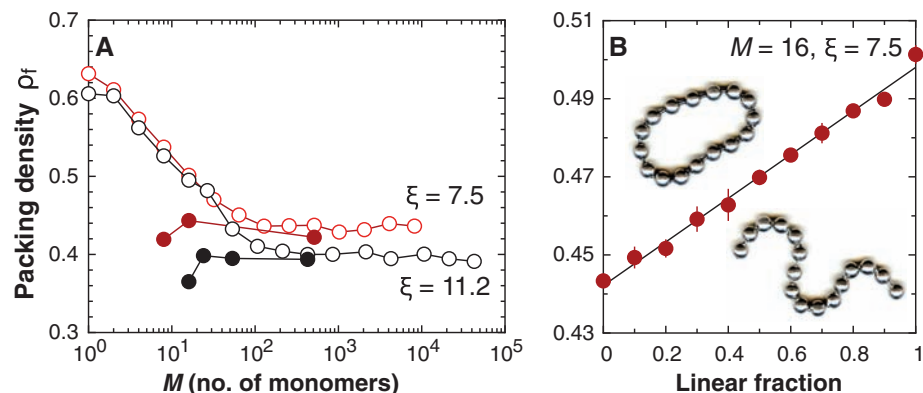


Fig. 1. (A) Packing density ρ_f of ball-chains versus chain length M after 10^4 taps, for both linear (open circles) and cyclic (solid circles) chains. Each data point is the average of five trials; error bars are smaller than the size of the symbols. (B) Packing density of a mixture of linear and cyclic chains (both with $M = 16$) as a function of the fraction of linear chains. Solid line is a linear fit.

¹The James Franck Institute and Department of Physics, University of Chicago, Chicago, IL 60637, USA. ²Department of Physics, Cornell University, Ithaca, NY 14853, USA. ³Department of Geophysical Sciences and Center for Advanced Radiation Sources, University of Chicago, Chicago, IL 60637, USA.

*To whom correspondence should be addressed. E-mail: zou@uchicago.edu

at $r/a = \sqrt{3}$ corresponds to a rhomboid cluster of four particles (Fig. 2A, inset); for chains, this requires contact between monomers without a shared bond. As we move to long chains, the $r/a = \sqrt{3}$ subpeak quickly disappears, indicating a sharp suppression in the number of contacts between monomers that do not share a bond. For spheres, the mechanical stability of the packing is provided by pair-wise contacts. For long chains, the suppression of pair-wise contacts between monomers that do not share a bond leaves the backbone as the remaining source of rigidity. But how can floppy chains be arranged into a rigid structure?

Unlike the $r/a = \sqrt{3}$ subpeak, the subpeak at $r/a = 2$ persists as M increases: It broadens and shifts slightly to $r < 2a$. This shift suggests that a large number of bonds must be flexed; for $M = 4096$, the peak center at $r/a = 1.89$ corresponds to a flex angle of 38° (Fig. 2B, inset). Measured directly, the flex angle distribution $p(\theta)$ for long chains ($M = 4096$) peaks strongly at $\theta_{\max} = 48^\circ$; in contrast, $p(\theta)$ for short chains ($M = 8$) is much flatter (Fig. 2C). We also compute the bond-orientational correlation $C_b(s - s')$ along a single chain

$$C_b(s - s') = \langle \vec{b}(s) \cdot \vec{b}(s') \rangle_s \quad (1)$$

Here, s and s' are monomer labels, and $\vec{b}(s)$ is the bond connecting monomers s and $s + 1$. Figure 2D shows $C_b(s - s')$ for compacted long chains. It decays rapidly from unity and becomes maximum anticorrelated at $s - s' \approx 6$ before returning to zero and executing small amplitude

oscillations (period $\approx 10.5a$). This observation indicates that there is no long-range orientational order along the backbone; instead, the local chain conformations contain a prevalence of near-minimal, semi-rigid loops (recall $\xi = 7.5$) (Fig. 3). For comparison, the $g(r)$ for $M = 8$ cyclic chains, which are rigid loops, is very similar to that for long chains, save for subtle differences: The second peak is sharper and is located at $r/a = 1.85$ (rather than 1.89), corresponding to next-nearest vertices of an octagon. The $g(r)$ of the $M = 16$ cyclic chain is nearly indistinguishable from that for long chains (Fig. 2B).

We suggest that these strongly flexed bonds and near-minimal loops are responsible for the rigidity of long-chain packings. Specifically, rigidity arises from the jamming of rigid elements (loops) that “condensed” out of a floppy object (the chain) upon compaction. Consider a pack of minimal loops, each with ξ monomers; these will be completely rigid rings. A ring has six degrees of freedom; for a pack of rings to be jammed (i.e., mechanically rigid), there must be on average six independent constraints per ring. These are provided by pair-wise contacts between rings. On jamming, each ring is on average in contact with 12 other rings; on a per-monomer basis, each monomer will have, on average, $12/\xi$ contacts or $z = 2 + 12/\xi$ nearest neighbors (coordination number). Compared with frictionless spheres, where the mean coordination at jamming is $z = 6$, a jammed pack of rigid rings is much less coordinated and therefore less densely packed. Because $z \sim 1/\xi$, the packing density will be even lower for stiffer chains (larger ξ).

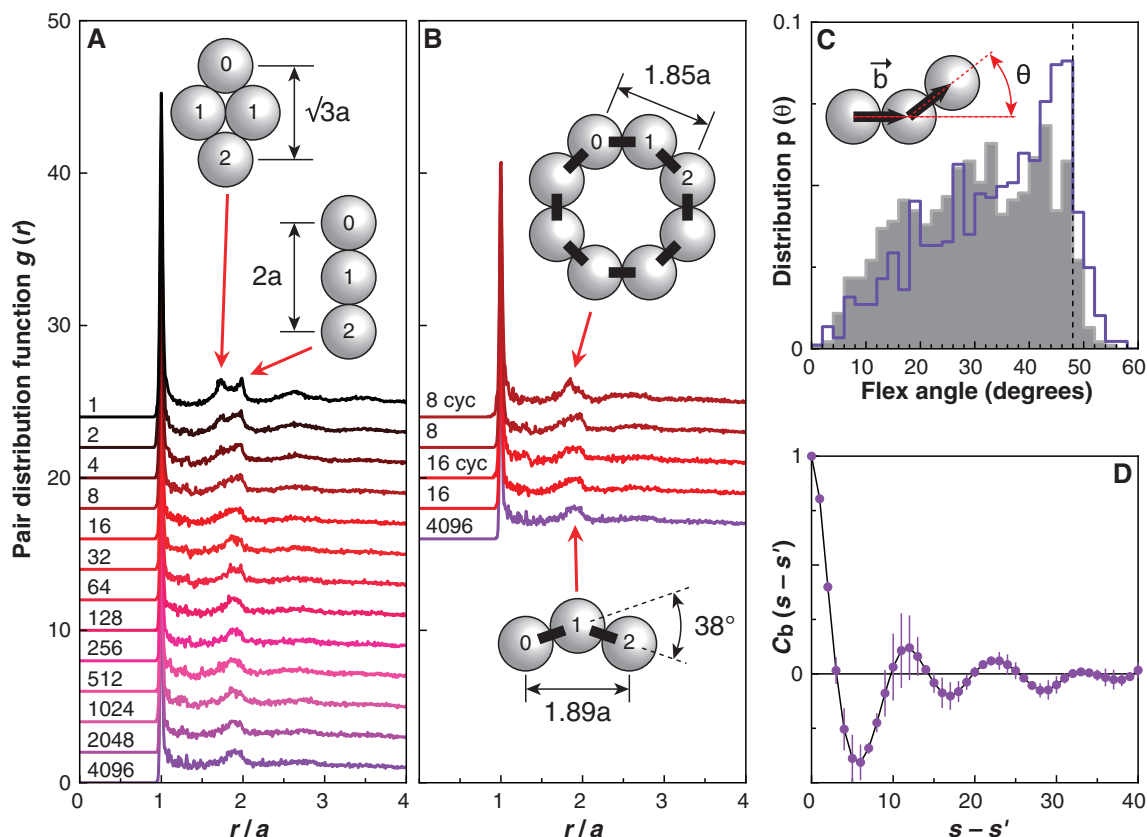
The loops in compacted chains are nearly, but not exactly, minimal in size; they are semi-rigid and have more degrees of freedom than do rigid rings. In addition, not all bonds are maximally flexed, and not all monomers belong on a loop. For linear chains, the chain ends, being bonded to only a single partner, are less constrained than monomers in the middle of a backbone. Each of these effects increases the number of constraints needed before a pack can jam, thereby enhancing the mean coordination and packing density at jamming. Therefore, we expect the following: (i) Long linear chains should pack less densely than short linear chains, but small, (nearly) rigid cyclic chains should pack the least densely of all. (ii) Stiff chains with large loop sizes should pack less densely than floppy chains with small ξ . Qualitatively, these statements agree with our experimental observations.

In the spirit of the jamming phase diagram (17), which links the glass transition of simple glass-formers with the jamming of grains, we suggest there is a similar connection between polymers and macroscopic chains. One well-studied aspect of the polymer glass transition is the variation of the glass transition temperature T_g on chain length and chain topology. For linear polymers, as $M \rightarrow \infty$, T_g quickly asymptotes to a constant value; whereas T_g decreases rapidly as $M \rightarrow 1$. This is commonly described by the Flory form

$$T_g = T_{g,\infty} - K/M \quad (2)$$

where $K > 0$ is a polymer-specific parameter (18). For cyclic polymers, in the long-chain limit, T_g is

Fig. 2. The pair distribution function $g(r)$ for compacted packing of chains ($\xi = 7.5$); curves are shifted for clarity. (A) Linear chains, from $M = 1$ to 4096. (B) Short cyclic (cyc) chains, compared with linear chains of the same length and also with a long linear chain. (C) The distribution of bond-flex angles for long ($M = 4096$, solid purple outline) and short ($M = 8$, gray shaded area) chain packings; the dashed vertical line indicates θ_{\max} . (D) The bond-orientational correlation $C_b(s - s')$ measured along a single chain, averaged over three long chain packings ($M = 1024, 2048, \text{ and } 4096$).



the same as that of long linear polymers of the same type, but as M becomes very small, T_g increases (19). As with ball-chains, the behavior of linear and cyclic polymers follows opposite trends as M becomes small.

The jamming phase diagram suggests a way to directly compare glassy polymers with jammed chains. Here, temperature T and specific packing volume $v \equiv 1/\rho$ are orthogonal axes; jammed/glassy states occupy the high-density, low-temperature region of the phase diagram, and fluid states occupy the rest. The glass transition is the transition from liquid to glass along the T axis, whereas jamming is the transition from unjammed to jammed states along the v axis at $T = 0$ (17). In this sense, $T_g(M)$ and $v_f(M) \equiv 1/\rho_f(M)$ should be analogous quantities. When we compare $T_g(M)/T_{g,\infty}$ for linear and cyclic poly(dimethylsiloxane) (PDMS) and $v_f(M)/v_{f,\infty}$ for the packing of chains, we see that there is a marked similarity between the two (Fig. 4).

As shown earlier, in a packing of floppy linear chains, chain ends act as non-interacting, density-enhancing defects. We can then write the specific packing volume v_f in the floppy regime as the weighted sum of v_e , contributed by ends, and $v_b > v_e$, due to the bulk

$$v_f(M) = \left(1 - \frac{2l}{M}\right)v_b + \left(\frac{2l}{M}\right)v_e = v_b - \frac{2l(v_b - v_e)}{M} \quad (3)$$

Here $l \sim \xi$ is the extent that end influences propagate into the bulk of the chain. Cast in this

Fig. 3. Tomographic reconstruction of a packing that consists of a single long chain ($M = 4096$). (A) The full reconstructed three-dimensional image. (B) A small slice of the packing, indicated by the shaded box in (A), projected onto the horizontal plane. The brighter a particle is, the closer it is to the center plane of the slice. Highlighted particles are arranged in three near-minimal loops.

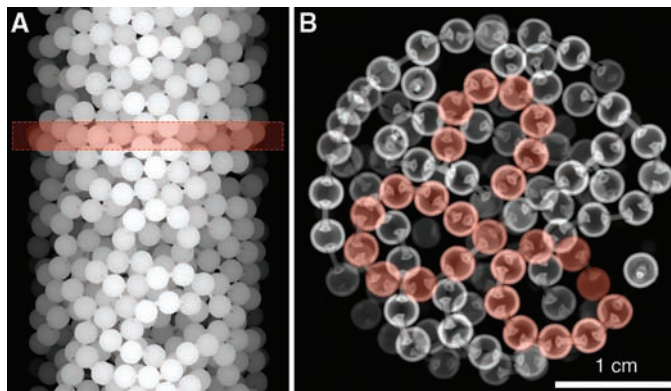
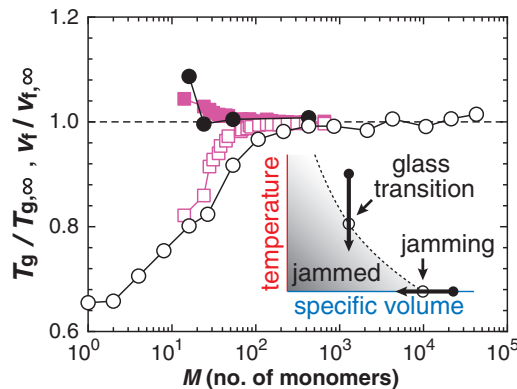


Fig. 4. The glass transition temperature $T_g(M)$ of linear and cyclic PDMS (open and solid squares) compared with the specific packing volume $v_f(M) \equiv 1/\rho_f(M)$ of linear and cyclic $\xi = 11.2$ ball-chains (open and solid circles). Both are normalized by their asymptotic $M \rightarrow \infty$ values $T_{g,\infty}$ and $v_{f,\infty}$. PDMS data are taken from (19). (Inset) The (T, v) plane of the jamming phase diagram, with trajectories for glass transition and jamming.



way, $v_f(M)$ takes on a form identical to the Flory form (Eq. 2) for $T_g(M)$. Fitted to appropriate regimes of the $\rho_f(M)$ data, we find for $\xi = 7.5$, $v_b = 2.3$ and $l(v_b - v_e) = 2.6$; taking $l = \xi = 7.5$, then $v_e = 1.95$. For $\xi = 11.2$, the best fit gives $v_b = 2.5$, and $l(v_b - v_e) = 6$; taking $l = \xi = 11.2$ gives $v_e = 1.96$.

Finally, chains with larger loop sizes pack less densely than chains with small ξ . The analogy of $v_f(M)$ with $T_g(M)$ suggests that stiff polymers will have a higher T_g than those that are more flexible. For vinyl polymers with rigid side groups that restrict chain flexibility, T_g is higher for those with large side groups than for those whose side groups are small (20).

These observations do not prove that the polymer glass transition must be attributable to the jamming of chains, especially at finite temperatures and with realistic interactions. The role of temperature points to important distinctions between polymers and ball-chains: (i) The stiffness of a ball-chain is given solely by its construction, but a polymer becomes stiffer at lower T , and (ii) for the packing of macroscopic objects, thermal motion is irrelevant, and the generalization of temperature is an open question (21). Therefore, the purely geometric jamming of chains cannot be exactly analogous to the glass transition in polymers. Some aspects of temperature can perhaps be simulated by varying the tapping strength used to compact the packing (6, 22). Interaction can also be introduced, for instance, by making the chains slightly sticky with a thin coating of viscous oil. But even for hard particles and no explicit tem-

perature, the similarities between jammed ball-chains and glassy polymers are pronounced enough to suggest that the jamming idea captures much of the physics. Because it has long been a matter of debate whether glass transitions in polymers and in simple glass-formers are fundamentally similar, it is attractive to think that jamming, whether of grains or chains, may provide a unifying connection.

We have shown that long, floppy chains pack into a low-density structure whose rigidity is chiefly provided by the backbone. This can be understood as the jamming of semi-rigid loops that formed when the chains were compacted. By invoking an analogy between the specific packing volume and the glass transition temperature, we have shown that the packing of chains parallels the polymer glass transition in important respects. If these two phenomena are indeed closely connected, as our data suggest, it would be a beautiful illustration of how molecular geometry and symmetry, independent of the specific microscopic interactions, can influence the structure of condensed matter.

References and Notes

1. T. Aste, D. Weaire, *The Pursuit of Perfect Packing* (Taylor & Francis, New York, ed. 2, 2008).
2. R. Zallen, *The Physics of Amorphous Solids* (Wiley-Interscience, New York, 1998).
3. J. D. Bernal, *Nature* **183**, 141 (1959).
4. G. D. Scott, *Nature* **194**, 956 (1962).
5. J. L. Finney, *Proc. R. Soc. London Ser. A* **319**, 479 (1970).
6. J. B. Knight, C. G. Fandrich, C.-H. Lau, H. M. Jaeger, S. R. Nagel, *Phys. Rev. E Stat. Phys. Plasmas Fluids Relat. Interdiscip. Top.* **51**, 3957 (1995).
7. F. X. Villarruel, B. E. Lauderdale, D. M. Mueth, H. M. Jaeger, *Phys. Rev. E Stat. Phys. Plasmas Fluids Relat. Interdiscip. Top.* **61**, 6914 (2000).
8. S. R. Williams, A. P. Philpse, *Phys. Rev. E Stat. Nonlin. Soft Matter Phys.* **67**, 051301 (2003).
9. A. Donev et al., *Science* **303**, 990 (2004).
10. W. Man et al., *Phys. Rev. Lett.* **94**, 198001 (2005).
11. Z. Zeravcic, N. Xu, A. J. Liu, S. R. Nagel, W. van Saarloos, *Europhys. Lett.* **87**, 26001 (2009).
12. M. Mailman, C. F. Schreck, C. S. O'Hern, B. Chakraborty, *Phys. Rev. Lett.* **102**, 255501 (2009).
13. R. W. Cahn, *Contemp. Phys.* **21**, 43 (1980).
14. R. L. Jernigan, P. J. Flory, *J. Chem. Phys.* **50**, 4178 (1969).
15. I. Carmesin, K. Kremer, *Macromolecules* **21**, 2819 (1988).
16. L. E. Silbert, A. J. Liu, S. R. Nagel, *Phys. Rev. E* **73**, 041304 (2006).
17. A. J. Liu, S. R. Nagel, *Nature* **396**, 21 (1998).
18. T. G. Fox, P. J. Flory, *J. Appl. Phys.* **21**, 581 (1950).
19. S. J. Clarson, K. Dodgson, J. A. Semlyen, *Polymer* **26**, 930 (1985).
20. A. Eisenberg, in *Physical Properties of Polymers*, J. E. Mark, Ed. (American Chemical Society, Washington, DC, ed. 2, 1993).
21. S. F. Edwards, D. V. Grinev, *Adv. Phys.* **51**, 1669 (2002).
22. E. R. Nowak, J. B. Knight, E. Ben-Naim, H. M. Jaeger, S. R. Nagel, *Phys. Rev. E Stat. Phys. Plasmas Fluids Relat. Interdiscip. Top.* **57**, 1971 (1998).
23. We thank P. Eng for his assistance and T. Witten for fruitful discussions. This work is supported by grants from NSF Materials Research Science and Engineering Center (DMR-0820054) and the U.S. Department of Energy (DOE) (DE-FG02-03ER46088). GSECARS is supported by grants from NSF (EAR-0622171) and DOE (DE-FG02-94ER14466). Use of the Advanced Photon Source is supported by DOE, Office of Science, Office of Basic Energy Sciences, under contract no. DE-AC02-06CH11357.

1 June 2009; accepted 1 September 2009
10.1126/science.1177114